Hindawi Publishing Corporation
Journal of Nanomaterials
Volume 2012, Article ID 384671, 6 pages
doi:10.1155/2012/384671

Research Article

Biocompatible Single-Crystal Selenium Nanobelt Based Nanodevice as a Temperature-Tunable Photosensor

Yongshan Niu,[1] Aimiao Qin,[2] Wei Song,[1] Menghang Wang,[1] Xuenan Gu,[1] Yangfei Zhang,[3] Min Yu,[3] Xiaoguang Zhao,[4] Ming Dai,[1] Ling Yan,[1] Zhou Li,[1] and Yubo Fan[1]

[1] *Key Laboratory for Biomechanics and Mechanobiology of Ministry of Education, School of Biological Science and Medical Engineering, Beihang University, Beijing 100191, China*
[2] *Key Lab of New Processing Technology for Nonferrous Metals & Materials Ministry of Education, School of Materials Science & Engineering, Guilin University of Technology, Guilin 541004, China*
[3] *College of Engineering, Peking Unversity, Beijing 100871, China*
[4] *Mechanical and Manufacturing Engineering, University of New South Wales, Sydney, NSW 2052, Australia*

Correspondence should be addressed to Zhou Li, lizhou@buaa.edu.cn and Yubo Fan, yubofan@buaa.edu.cn

Received 1 March 2012; Accepted 19 March 2012

Academic Editor: Xiaoming Li

Selenium materials are widely used in photoelectrical devices, owing to their unique semiconductive properties. Single-crystal selenium nanobelts with large specific surface area, fine photoconductivity, and biocompatibility provide potential applications in biomedical nanodevices, such as implantable artificial retina and rapid photon detector/stimulator for optogenetics. Here, we present a selenium nanobelt based nanodevice, which is fabricated with single Se nanobelt. This device shows a rapid photo response, different sensitivities to visible light of variable wave length, and temperature-tunable property. The biocompatibility of the Se nanobelts was proved by MTT test using two cell lines. Our investigation introduced a photosensor that will be important for multiple potential applications in human visual system, photocells in energy or MEMS, and temperature-tunable photoelectrical device for optogenetics research.

1. Introduction

One-dimensional (1D) nanostructures such as nanowires [1, 2], nanobelts [3], and nanotubes [4] showed their fascinating features and characteristic during the past few decades. Intensive researches focused on their applications in microcosmic physics and nanodevices [5–8]. Selenium material is a crucial semiconductor, widely used in solar cell, photoelectrical element, xerography, and pressure sensors, owing to its unique photoconductivity, thermoelectric, and piezoelectric properties [9–16]. Previously, most research about the selenium mainly focused on bulk or amorphous materials and hexagonal metallic selenium film.

Recently, the 1D selenium nanostructures, such as single-crystalline nanowires [16, 17] and nanobelts [18], become a new research focus. Numerous works are about synthesis of 1D selenium nanostructures. However, the study about their properties and applications in photoelectrical nanodevices is limited. Meanwhile, the biocompatibility and biosafety of nanostructure is also a serious public concern.

A new single-crystalline selenium nanobelt based photosensor is presented here. This single nanobelt device exhibits ultrafast photon response and temperature-tunable properties. We used a cushy and large-scale synthesis method to prepare the single-crystalline nanobelts and investigated their cellular level biocompatibility to two different cell lines. This photosensor also presented a variable photoconductivity responding to visible light of different wavelengths. Those novel properties endue the nanodevice multiple potential applications, such as implantable visual nanodevice as artificial retina, rapid photon sensors, photocells, or temperature-tunable photoelectrical element.

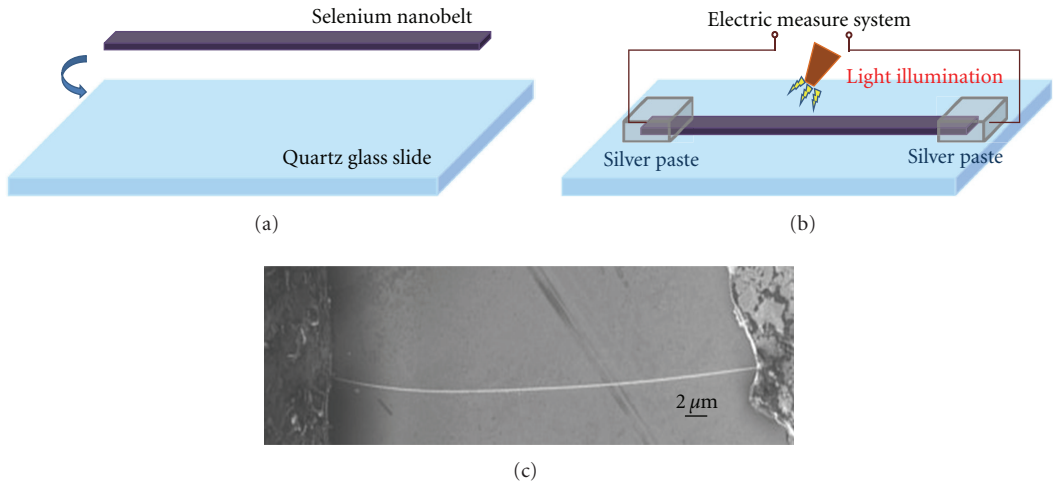

Figure 1: Fabrication of a single selenium nanobelt nanodevice. (a) Transfer a single selenium nanobelt to a cleaned quartz glass slide. (b) Fix both ends of nanobelt by silver paste through suitable masks and connect with electric measure system by enameled copper wire. (c) The SEM image of fabricated nanodevice. Two ends are silver pasted, and the bright line is a Se nanobelt.

2. Experiment

2.1. Synthesis. Single-crystalline t-selenium nanobelts were synthesized by solventothermal method. A typical experimental procedure is described as following: 1.3 mmol (0.1 g) Se powder and 17 mL ethanol were loaded into teflon-lined autoclave of 25 mL capacity. This autoclave was sealed and maintained at 200°C for 24 h. Then the autoclave was taken out and cooled in room temperature. Precipitates were filtered out, rinsed with absolute alcohol for several times, and dried naturally. All of chemicals used for the synthesis were of analytical grade and used as received without further purification.

2.2. Characterization and Fabrication. The synthesized selenium nanobelts were characterized and analyzed by X-ray diffraction (XRD, Alpha-1) using CuKa radiation, SEM (FE-SEM, Leon 1530 with EDS), and TEM (TEM, HF-2000).

A single selenium nanobelt was transferred to a cleaned quartz glass slide to fabricate a nanodevice. Both ends of the Se nanobelt were fixed by silver paste and connected with copper wire (Figure 1). The electronic transportation property was conducted on the single nanobelt device by an electric measure system. Besides, we used fluorescent lamp, ultraviolet lamp, and photoluminescence measure instrument to investigate the photoconductivity of the device. The electric property was measured in constant temperature environment. All measurement was carried out and recorded by same electric measure system.

2.3. Biocompatibility Test. For our study, two cell lines were utilized [19, 20]. One was HeLa cell (American Type Culture Collection, ATCC, CCL-2) and the other one was L-929 cell (ATCC, CCL-1). Two kind of cells were cultured in Dulbecco's modified Eagle's medium (DMEM, ATCC) supplemented with 10% fetal bovine serum (FBS, ATCC) and 1% penicillin/streptomycin (ATCC). Cell suspension was added to 25 cm^2 vials and put into an incubator (37°C, 5% CO_2).

After being incubated for 24 h, cells were trypsinized with 0.05% trypsin solution and rushed down from the bottom of 25 cm^2 vials when they were in a semiconfluent state and still in log phase of growth. Ten microliter cell suspension was mixed with 10 μL trypan blue, and the total number of harvest cells was counted under an optical microscope. The density of the cell was calculated and cellular viability was greater than 90%. The cell suspension was added to 96-well plates with 5000 cells per well (90 μL). 96-well plates were incubated in 37°C, 5% CO_2 for 12 h.

Se nanobelts were suspended in PBS (10 μL) for four different concentrations. These suspensions were added into 96-well plates until the mass concentration of 0.1, 1, 10, and 100 μg/mL, respectively. Some wells were preserved without adding nanobelts for comparison purpose. After dispersing nanobelts by micropipettes, the 96-well plates were incubated in 37°C, 5% CO_2 for 12, 24, and 48 h, respectively.

The biocompatibility of the Se nanobelt was investigated through an in vitro cell viability test. We measured the activity of mitochondrial enzyme succinate dehydrogenase (SDH) [21] in two different cell lines, after adding Se nanobelts and incubating for 12, 24, and 48 h.

The Se nanobelts were not removed from each well and an MTT (3-[4,5-dimethyl-thiazol-2-yl]-2,5-diphenyl tetrazolium bromide)-succinate solution (20 μL, 0.5 mg/mL MTT) was added, and the plates were incubated again at 37°C for 4 h. Then all solution in the 96-well plates was removed. The MTT-formazan formed by the mitochondrial enzyme SDH was preserved at the bottom of the well and dissolved in added dimethyl sulfoxide (DMSO). The 96-well plates were shaken softly for 5 minutes to dissolve formazan absolutely. Then the plates were put in a microplate reader

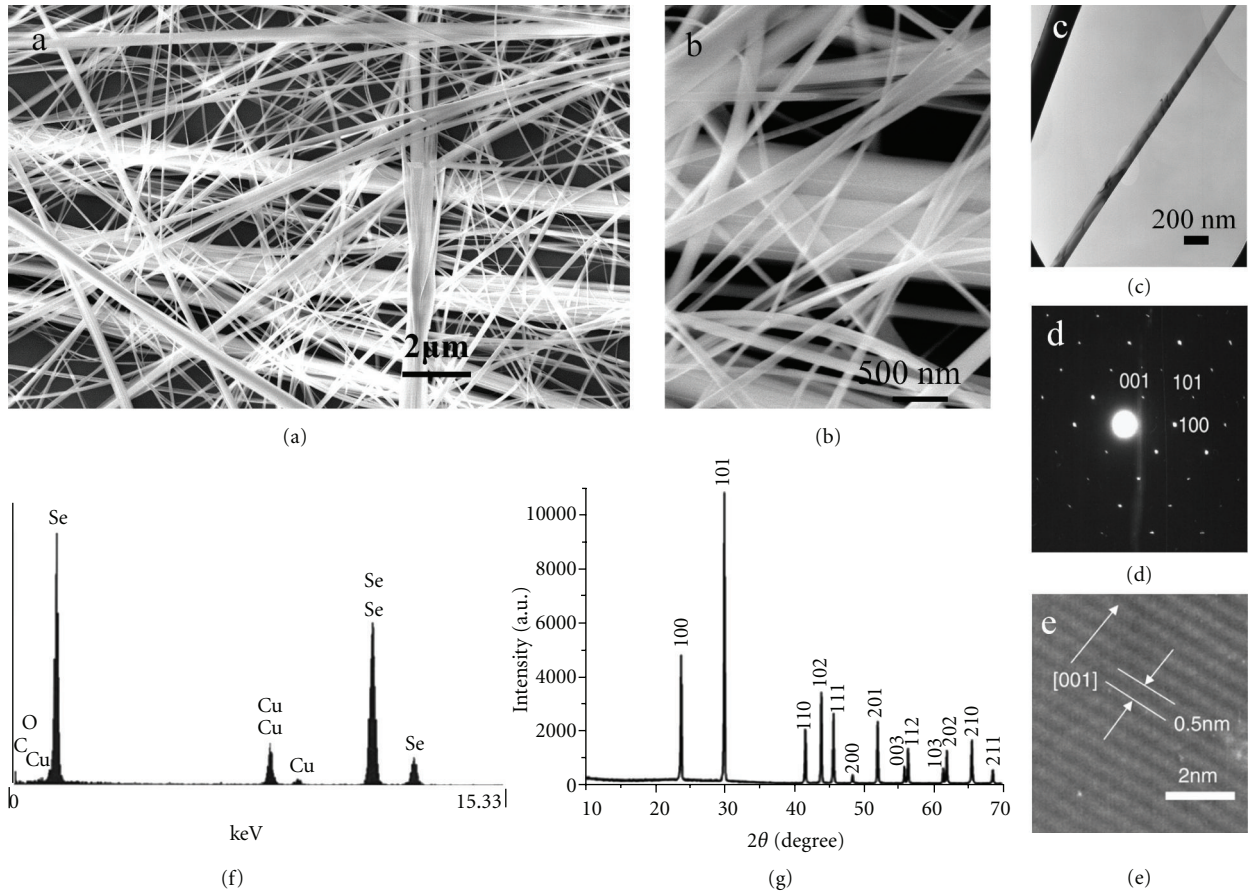

Figure 2: SEM, HRTEM, EDS, and XRD characterization of selenium nanobelts. ((a), (b)) SEM images of single-crystalline Se nanobelts in different magnifications. ((c)–(e)) HRTEM images taken from the middle of the Se nanobelt show that the corresponding electron diffraction pattern and its growth direction is [001]. (f) EDS indicates the Se nanobelts with pure composition. (g) XRD pattern confirms that the Se nanobelts are trigonal structure.

(EL808 IU-PC, BioTek Instruments, Inc.), recording the photon absorbance of each well at 630 nm wavelength for investigating the viability of cells.

3. Results and Discussion

As shown in the SEM images of different magnifications, the size range of the t-Se nanobelts was from 100 to 500 nm in width and tens to hundreds of micrometers in length. The ratio of length to diameter was $10^2 \sim 10^4$ (Figures 2(a) and 2(b)). We did chemical element analysis using EDS to test the purity of Se nanobelt (Figure 2(f)). The XRD showed the structure of Se nanobelt is trigonal (Figure 2(g)). And HRTEM study further confirmed that the t-Se nanobelts had single-crystal structure with growth direction [001] (Figures 2(c), 2(d), and 2(e)).

In MTT test, we found that single-crystal Se nanobelts are biocompatible and biosafe to the two cell lines (Figure 3). Our investigation was designed by time sequence and concentration. The incubation time was 12, 24, and 48 h, and the concentration was 10^{-3}, 10^{-2}, 0.1, and 1 mg/mL. The viability of HeLa and L929 cells showed no difference comparing with control after incubating with nanobelts. More than 85% of the HeLa cells and >80% L929 cells were viable after incubation, and there was no significant statistic difference in viability among the plates of time sequence (tested by SPSS, paired-sample t-test). Meanwhile, different concentrations of Se nanobelts showed no significant effect to the viability of HeLa and L929 cells too (Figure 3).

A single-crystal selenium photosensor device was fabricated (Figure 1). Two ends of the Se nanobelt were fixed by silver paste. The electrical measurement system was connected with the device through enameled copper wires. The photoconductivity measurement was first performed in room temperature and room light (fluorescent lamp). The response time of the Se nanobelt to visible light is calculated. With the light turned on and off, the current changed immediately. From the I-t curve, it is observed that the current transported through a single nanobelt drastically increases by a factor of 10 when the light was turned on. As measured at half maximum from I-t curve, the increasing and the decay response time was about 30 and 50 ms, respectively. This nanobelt based nanodevice presented a high sensitivity and rapid response to light at room temperature.

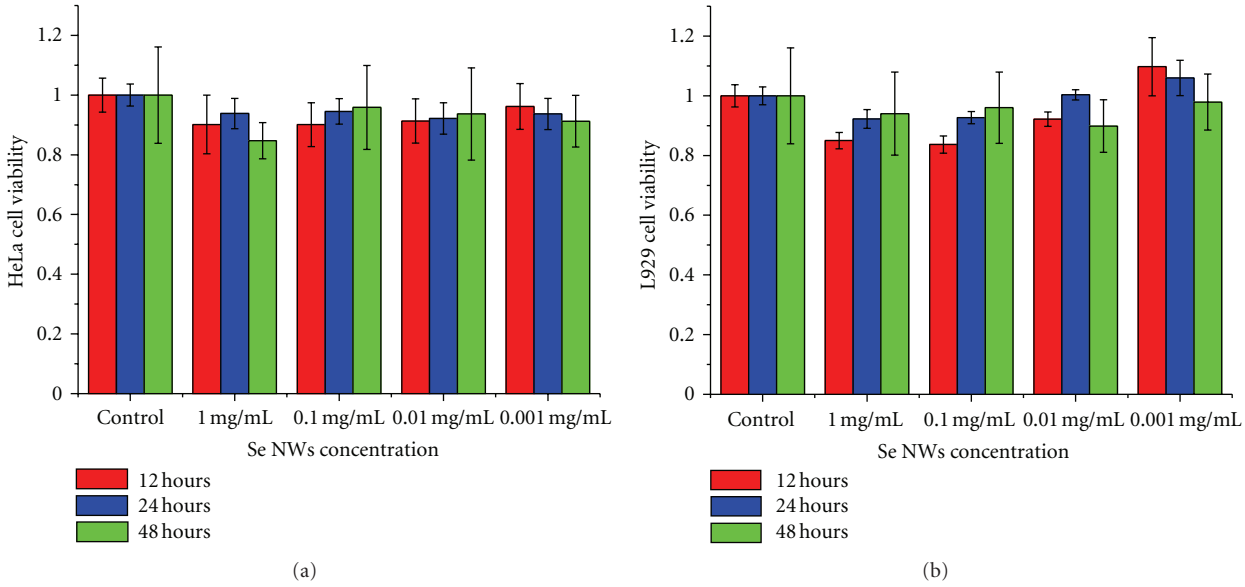

Figure 3: The cell viability tested by MTT method as a function of Se nanobelt concentration and time. (a) Cell viability of HeLa cells in MTT test, cultured with different concentrations of Se nanobelts for 12, 24, and 48 h. (b) Viability of L929 cells in MTT test, cultured with different concentrations of Se nanobelts for 12, 24, and 48 h.

This nanobelt based photosensor also exhibited a temperature-tunable property (Figure 4(a)). In this experiment, we changed environmental temperature from −80°C to 80°C. The voltage was applied to 1 V. The current change in volume reduced with the temperature rise. In semiconductive material, the conductivity is mainly determined by the recombination and trapping of the electron-hole pairs. Generally, when temperature rises, the rate of recombination and trapping increases, displayed as the increasing of conductivity in semiconductor. This trigonal selenium was accepted as a p-type extrinsic semiconductor, and conduction occurred due to valence band hole transportation [22]. The increased thermal conductivity was likely due to the thermal excitation of the electron-hole pairs in the valence band as governed by $\exp(-E_g/KT)$, where $E_g = 1.6$ eV was the bandgap of selenium, K is Boltzmann constant, and T is temperature.

The rate of recombination and trapping in this selenium nanobelt was shown strongly depending on light and temperature [22, 23]. The photosensitivity, defined as $S = (I - I_o)/I_o$ where I and I_o were the currents measured when the light was on and off, respectively, was strongly affected by temperature. S decreased as temperature increased. In our experiment, the best photosensitivity was received at temperatures lower than 40°C. The carriers in Se nanobelt were contributed by photon excitation and thermal excitation. With the temperature increasing, the thermal excitation was enhanced and the photosensitivity was relatively reduced. This property of the nanodevice was a temperature-tunable ability, which was likely to be important for the applications in human visual system, implantable light-adjusted medical devices, and the new scientific field of optogenetics [24–26].

In order to investigate the photon sensitivity of the Se nanobelt to the light of different wavelengths, the photocurrent was measured under a chopped light (75 Watt xenon lamp) to give monochromatic light. The wave length was set from UV to infrared light (300 to 800 nm). I-t curve showed a significant result as the photosensor's response (Figure 4(b)). The higher response was observed in the visible wave length, which was in agreement with the previous report [12]. This was attributed to the particular photo character of Se nanobelts with some other semiconductors, such as ZnO nanobelts [27, 28]. The maximum photo response of our single-crystal t-Se nanobelt was at ~650 nm in room temperature, which was a little different with previous report: 650 nm at −190°C and 750 nm at 20°C [28]. The sensitive response to visible light and temperature-tunable ability was superiority for this Se nanobelt based photosensor applied in implantable biomedical device, such as artificial retina and the optogenetics detector/stimulator.

4. Conclusion

In summary, we synthesized and characterized the single-crystal selenium nanobelts. We also investigated their biocompatibility to different cells. The viability of cells incubated with Se nanobelts showed no difference with the control. More than 80% cells were viable indicating the Se nanobelts behaving a good biocompatibility and biosafety. A photoelectrical nanodevice was fabricated here, and it showed a significant result to visual light of different wavelengths. Moreover, this photosensor exhibited a temperature-tunable ability. As a conclusion, this biocompatible single-crystal Se nanobelt based temperature-tunable photosensor seems to be important for multiple potential applications, such as artificial retina for human visual system, photocells in energy or MEMS, and temperature-tunable photoelectrical device for optogenetics research.

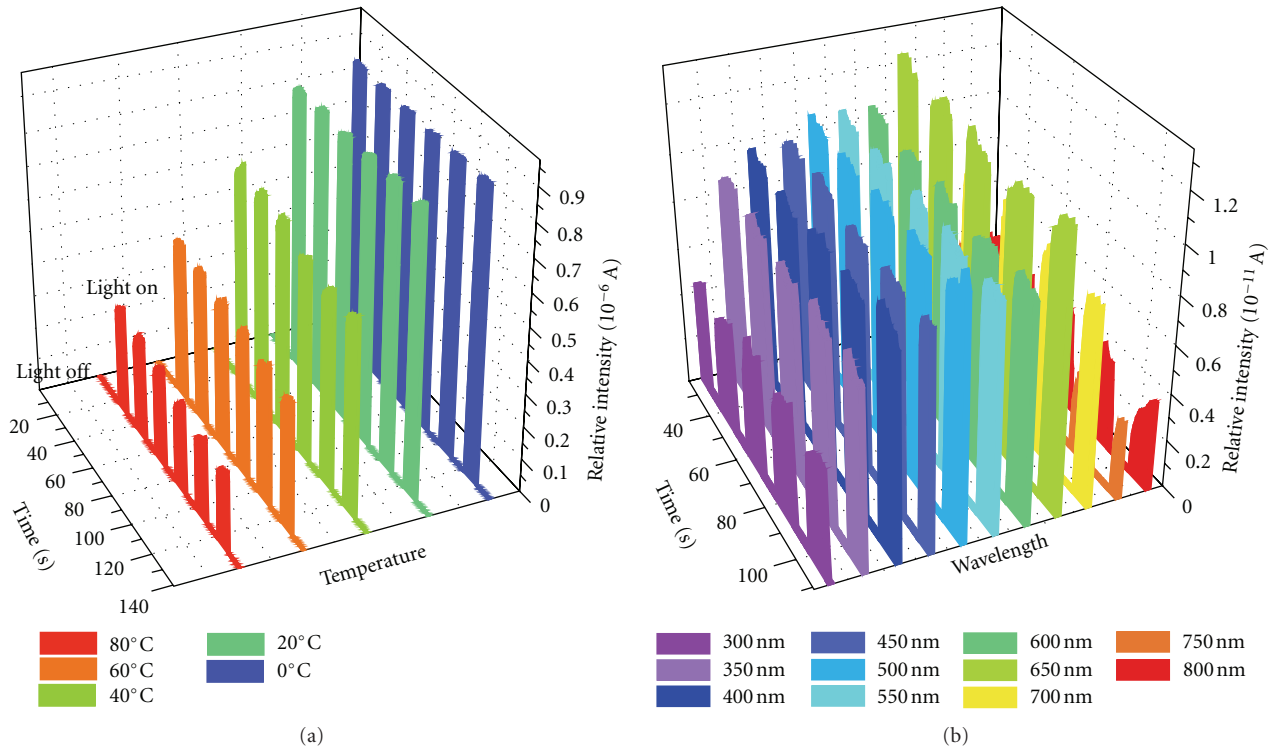

FIGURE 4: The I-t curve of Se nanobelt based photosensor. (a) The temperature-tunable property of our photosensor. Relative current intensity defines as $(I - I_0)$. Temperature changes from 0°C to 80°C. (b) Our photosensor presents sensitive response to the light of different wavelengths, from 300 nm to 800 nm.

Acknowledgments

This work was supported under the Scientific Research Foundation for the Returned Overseas Chinese Scholars (20091341) and the Doctoral Fund of the Ministry of Education of China (20111102120038), the National Natural Science Foundation of China (no. 10925208) and NSF of Guangxi Province (2010GXNSFC013007), and National Basic Research Program of China (973 Program, 2011CB710901). Z. Li also thanks the support from the Excellent Scientist Program of the Beihang University. Yongshan Niu and Aimiao Qin are equally contributed to this paper.

References

[1] Y. Cui, L. J. Lauhon, M. S. Gudiksen, J. Wang, and C. M. Lieber, "Diameter-controlled synthesis of single-crystal silicon nanowires," *Applied Physics Letters*, vol. 78, no. 15, pp. 2214–2216, 2001.

[2] Z. L. Wang and J. H. Song, "Piezoelectric nanogenerators based on zinc oxide nanowire arrays," *Science*, vol. 312, no. 5771, pp. 242–246, 2006.

[3] Z. W. Pan, Z. R. Dai, and Z. L. Wang, "Nanobelts of semiconducting oxides," *Science*, vol. 291, no. 5510, pp. 1947–1949, 2001.

[4] S. Iijima, "Helical microtubules of graphitic carbon," *Nature*, vol. 354, no. 6348, pp. 56–58, 1991.

[5] Z. Li, G. Zhu, R. S. Yang, A. C. Wang, and Z. L. Wang, "Muscle-driven in vivo nanogenerator," *Advanced Materials*, vol. 22, no. 23, pp. 2534–2537, 2010.

[6] P. H. Yeh, Z. Li, and Z. L. Wang, "Schottky-gated probe-free ZnO nanowire biosensor," *Advanced Materials*, vol. 21, no. 48, pp. 4975–4978, 2009.

[7] X. Li, C. A. van Blitterswijk, Q. Feng, F. Cui, and F. Watari, "The effect of calcium phosphate microstructure on bone-related cells in vitro," *Biomaterials*, vol. 29, no. 23, pp. 3306–3316, 2008.

[8] X. M. Li, H. F. Liu, X. F. Niu et al., "Osteogenic differentiation of human adipose-derived stem cells induced by osteoinductive calcium phosphate ceramics," *Journal of Biomedical Materials Research B*, vol. 97, no. 1, pp. 10–19, 2011.

[9] X. M. Li, H. F. Liu, X. F. Niu et al., "Osteogenic differentiation of human adipose-derived stem cells induced by osteoinductive calcium phosphate ceramics," *Journal of Biomedical Materials Research B*, vol. 97, no. 1, pp. 10–19, 2011.

[10] J. A. Johnson, M. L. Saboungi, P. Thiyagarajan, R. Csencsits, and D. Meisel, "Selenium nanoparticles: a small-angle neutron scattering study," *Journal of Physical Chemistry B*, vol. 103, no. 1, pp. 59–63, 1999.

[11] R. A. Zingaro and W. C. Cooper, Eds., *Selenium*, Van Nostrand Rainhold, New York, NY, USA, 1974.

[12] L. I. Berger, *Semiconducting Materials*, CRC Press, Boca Raton, Fla, USA, 1997.

[13] B. Gates, B. Mayers, A. Grossman, and Y. Xia, "A sonochemical approach to the synthesis of crystalline selenium nanowires in solutions and on solid supports," *Advanced Materials*, vol. 14, pp. 1749–1752, 2002.

[14] U. K. Gautam, M. Nath, and C. N. R. Rao, "New strategies for the synthesis of t-selenium nanorods and nanowires," *Journal of Materials Chemistry*, vol. 13, no. 12, pp. 2845–2847, 2003.
[15] H. T. Li and P. J. Regensburger, "Photoinduced discharge characteristics of amorphous selenium plates," *Journal of Applied Physics*, vol. 34, no. 6, pp. 1730–1735, 1963.
[16] B. Gates, B. Mayers, B. Cattle, and Y. Xia, "Synthesis and characterization of uniform nanowires of trigonal selenium," *Advanced Functional Materials*, vol. 12, no. 3, pp. 219–227, 2002.
[17] B. T. Mayers, K. Liu, D. Sunderland, and Y. Xia, "Sonochemical synthesis of trigonal selenium nanowires," *Chemistry of Materials*, vol. 15, no. 20, pp. 3852–3858, 2003.
[18] Q. Wang, G. D. Li, Y. L. Liu, S. Xu, K. J. Wang, and J. S. Chen, "Fabrication and growth mechanism of selenium and tellurium nanobelts through a vacuum vapor deposition route," *Journal of Physical Chemistry C*, vol. 111, no. 35, pp. 12926–12932, 2007.
[19] C. T. Hanks, J. C. Wataha, and Z. Sun, "In vitro models of biocompatibility: a review," *Dental Materials*, vol. 12, no. 3, pp. 186–193, 1996.
[20] Z. Li, R. Yang, M. Yu, F. Bai, C. Li, and Z. L. Wang, "Cellular level biocompatibility and biosafety of ZnO nanowires," *Journal of Physical Chemistry C*, vol. 112, no. 51, pp. 20114–20117, 2008.
[21] J. C. Wataha, R. G. Craig, and C. T. Hanks, "Precision of and new methods for testing in vitro alloy cytotoxicity," *Dental Materials*, vol. 8, no. 1, pp. 65–70, 1992.
[22] W. E. Spear, "Carrier mobility and charge transport in monoclinic Se crystals," *Journal of Physics and Chemistry of Solids*, vol. 21, no. 1-2, pp. 110–IN1, 1961.
[23] M. A. Gilleo, "Optical absorption and photoconductivity of amorphous and hexagonal selenium," *The Journal of Chemical Physics*, vol. 19, no. 10, pp. 1291–1297, 1951.
[24] G. Miller, "Shining new light on neural circuits," *Science*, vol. 314, no. 5806, pp. 1674–1676, 2006.
[25] D. L. McLean and J. R. Fetcho, "Movement, technology and discovery in the zebrafish," *Current Opinion in Neurobiology*, vol. 21, no. 1, pp. 110–115, 2011.
[26] G. Miesenbock, "The optogenetic catechism," *Science*, vol. 326, no. 5951, pp. 395–399, 2009.
[27] J. H. He, Y. H. Lin, M. E. McConney, V. V. Tsukruk, Z. L. Wang, and G. Bao, "Enhancing UV photoconductivity of ZnO nanobelt by polyacrylonitrile functionalization," *Journal of Applied Physics*, vol. 102, no. 8, Article ID 084303, 2007.
[28] D. S. Elliott, "A comparative study of the light-sensibility of selenium and stibnite at 20°C. and-190°C," *Physical Review*, vol. 5, no. 1, pp. 53–64, 1915.